

Atomic mixing and interface reactions in Ta/Si bilayers during noble-gas ion irradiation

S. Dhar,^{1,*} M. Milosavljevic,^{1,2} N. Bibic,^{1,2} and K. P. Lieb¹¹*II. Physikalisches Institut and Sonderforschungsbereich 345, Universität Göttingen, Bunsenstrasse 7-9, D-37073 Göttingen, Germany*²*VINCA Institute of Nuclear Science, Belgrade, Yugoslavia*

(Received 3 June 2001; revised manuscript received 12 October 2001; published 19 December 2001)

This article focuses on the influence of chemical driving forces on the mixing and phase formation taking place at the interface of highly reactive metal/semiconductor systems under ion-beam irradiation. Ta/Si bilayers were irradiated with Ar, Kr, and Xe ions to fluences of $(0.5-2.5) \times 10^{16}$ ions/cm² and at temperatures between liquid nitrogen and 400 °C. The interface mixing and silicide formation were monitored as function of the ion mass and fluence by means of Rutherford backscattering spectrometry and x-ray diffraction. The interface broadening variance was found to depend linearly on the ion fluence and was explained with the help of a compound formation model involving local or global thermal spikes. The results are compared with those found in other silicide and germanide systems. The transition from local to global spikes was found to occur at the critical deposited damage energy of about 2.5 keV/nm.

DOI: 10.1103/PhysRevB.65.024109

PACS number(s): 61.80.-x, 68.55.Ln, 85.40.Ry

I. INTRODUCTION

Transition- and refractory-metal silicides are potentially attractive materials for various applications.¹ These silicides have many interesting physical and chemical properties, such as low resistivity, semiconducting behavior with direct and indirect band gaps, high-temperature chemical stability, small lattice mismatch with Si, and oxidation resistance.²⁻⁴ Compared to noble-metal silicides, the application of refractory silicides, such as WSi₂ or TaSi₂, appears more useful in high-temperature environments. Ion-beam techniques such as ion implantation and ion-beam mixing are very attractive as they allow one to process the materials at comparatively low temperatures and in fewer processing steps, although problems may arise from the implanted species.

In the last two decades, much attention has been devoted to understanding the ion-induced atomic transport processes and phase formation across metal/Si, Si/silicide, and metal/silicide interfaces.^{1,2,5-7} During irradiation, heavy ions locally deposit large amounts of energy and induce strong atomic diffusion, leading to interface mixing and chemical reactions.⁷⁻¹¹ Elevated temperatures during irradiation further enhance these processes. It has been demonstrated that the thermal spikes and chemical driving forces enhance atomic mixing during ion irradiation.^{8,9} The thermal spike, which is defined as the localized increase of very high temperature for a short duration of time, can be either local⁸ or global⁷⁻⁹ in nature, depending on the amount of the deposited damage energy F_D by the incident ion. Local spikes are formed inside the isolated collisional subcascades below a critical F_D value. Above this value, all collisional subcascades overlap and produce a global spike. The phase structure of the modified region is either a solid solution or a compound phase or a mixture of both. Ion-induced mixing in the case of solid solutions, i.e., atomic transport through the interface(s) of bi- and multilayers can be rather well modeled in many systems. On the other hand, the transition to phase formation, the growth mechanisms of phases, the relationship to the mixing process (ballistic or thermal spike mixing,

radiation-enhanced diffusion), and the individual contributions of ion-induced and thermal processes are not well understood yet.¹⁰⁻¹⁴ For this reason, we have extended previous studies on metal/Si and nitride/Si bilayer systems¹⁴⁻¹⁸ to the Ta/Si system. In this paper we present a comprehensive investigation, in which we varied the energy deposited at the interface by either changing the target thickness or ion mass (Ar, Kr, Xe), and the substrate temperature (liquid-nitrogen temperature up to 400 °C). A detailed analysis within various mixing models has enabled us to explain the experimental results of Ta/Si system. The present results and those obtained for other highly reactive metal/semiconductor bilayers^{10-13,18} clearly show the requirement of either local or global thermal spikes in the formation and growth of silicide or germanide phases. A critical deposition energy for the transition from local spikes (Ar) to global spikes (Kr, Xe) has been found.

II. EXPERIMENTAL METHODS

Ta films of 30–70 nm thickness were deposited by dc magnetron sputtering in an Ar atmosphere on Si(100) wafers. Before deposition, the Si surface was first cleaned in an HF solution and then by 1.5-keV Ar-ion sputtering inside the deposition chamber. It should be noted that a few nm (3–4 nm) of the top Si layers might be amorphized during this Ar cleaning process. The deposition rate was maintained at 8–10 nm/min and the substrates were kept at room temperature (RT) during deposition. The ion irradiations were performed at various energies: (i) 120 keV Ar, (ii) 400 keV Kr, and (iii) 475 keV Xe using the TESLA facility at Vinca¹⁹ and the 500-kV Göttingen ion implanter IONAS.²⁰ The combinations of ion energy and thickness of the Ta film were chosen in such a way that a large damage energy was deposited at the Ta/Si interface. In all the cases, the fluence of the implanted ions was varied in the range of $(0.5-2.5) \times 10^{16}$ ions/cm². The sample temperature during irradiation varied between liquid-nitrogen temperature (LN₂) and 400 °C. The beam current was maintained at around 1

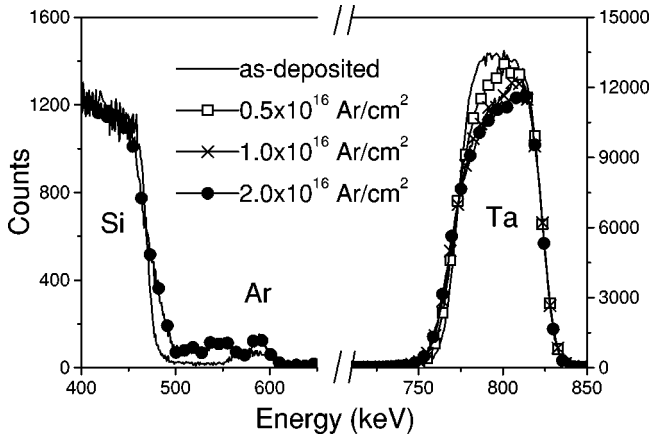


FIG. 1. RBS spectra taken before and after 120-keV Ar-ion irradiation of Ta (47 nm)/Si bilayers at RT. The Ta signals and the signals corresponding to Si and Ar are plotted in different scales.

$\mu\text{A}/\text{cm}^2$ in order to avoid beam heating. The TRIM95 code²¹ was used to simulate the ion range and the deposited energy distributions by considering a detailed calculation of secondary collision cascades.

Due to the large mass difference of the components, Rutherford backscattering spectrometry (RBS) was suitable to monitor the ion-induced transport across the interface as well as the accumulation of the implanted ions in the substrate. For taking the RBS spectrum,²² the 900-keV He^{2+} ion beam of IONAS was used. Two surface barrier detectors positioned at a 165° backscattering angle with a detector resolution of 13.5 keV [full width at half maximum (FWHM)] were employed for the data collection. The Ta and Si depth profiles were extracted from the RBS spectra by means of the RUMP (Ref. 23) and WINDF (Ref. 24) codes. The phase structure of the intermixed region was monitored via 3° -grazing-angle x-ray diffraction (XRD) using the Cu ($K\alpha$) line.

III. EXPERIMENTAL RESULTS

A. 120-keV Ar-ion irradiation

Ta films of 30, 47, and 67 nm thickness were used for studying the ion-beam mixing via 120-keV Ar ions at RT. These experiments were specifically designed to vary the energy deposited at the Ta/Si interface. Figure 1 shows a set of RBS spectra taken from the 47-nm Ta/Si system before and after irradiation at different Ar-ion fluences. For the sake of clarity, we have presented the RBS signals of Ta (right) and of Si and the implanted Ar (left) in different scales. It is clearly visible that the Ta yield loses height and spreads at the interface with increasing ion fluence Φ . The estimated surface sputtering is at a rate of around 1 Ta atom/Ar ion. Interface broadening is also visible in the Si distributions. The implanted Ar concentration builds up in the form of two peaks, one positioned within the Ta-rich region and the other one reaching deeper into the Si substrate. A detailed analysis showed that about 4 at. % of Ar was incorporated during the sputter cleaning process of Si and Ta deposition prior to the Ar-ion irradiation.

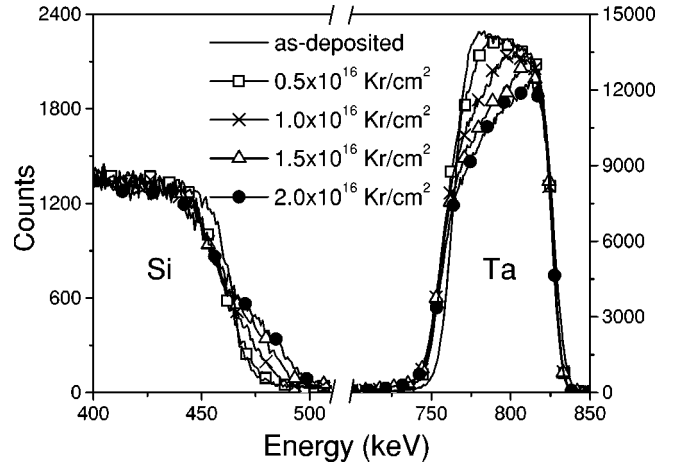


FIG. 2. RBS spectra taken before and after 400-keV Kr-ion irradiation of Ta (47 nm)/Si bilayers at RT. The implanted Kr signals are not shown in the figure.

Similar results were obtained for the case of 30- and 67-nm-thick Ta layers. The mixing effects for the 30-nm Ta/Si sample are larger than those for the 67-nm Ta/Si sample because the deposited energy (F_D) of 0.47 keV/nm for the 30-nm Ta/Si sample is higher than the value $F_D = 0.3$ keV/nm calculated for the 67-nm Ta/Si sample. Since the sputtered thickness of the Ta layer is very small, the deposition energy across the interface remains more or less constant.

B. 400-keV Kr-ion irradiation

400-keV Kr-ion irradiations were performed for 47-nm Ta/Si samples at LN_2 and RT. Figure 2 shows the RBS spectra obtained from the samples irradiated at RT. The concentration profiles of Ta and Si were extracted using the RUMP code²³ and are plotted in Fig. 3. As in the case of Ar irradiation, the interdiffusion of Ta and Si across the interface increases progressively with the fluence Φ . However, in this case the mixing rate is expected to be higher since the deposited energy $F_D = 2.5$ keV/nm is much larger than in the case of Ar irradiation. At a fluence of 2×10^{16} ions/ cm^2 , Si has diffused almost up to the surface. Similar results were obtained for irradiations at liquid-nitrogen temperature. The analyses indeed show that mixing and interdiffusion are almost independent of the irradiation temperature in the range 100–300 K.

C. 475-keV Xe-ion irradiation

Xe-ion irradiations of 67-nm Ta/Si samples were performed at different temperatures in the range LN_2 to 400°C . The RBS spectra taken after Xe irradiation at RT and LN_2 and for different fluences show features similar to those of Ar and Kr irradiation. In all of the above cases, we have seen that the initially well-separated Ta and Si profiles gradually become mixed with increasing ion fluence and in general develop into nonhomogeneous distributions. The formation of a homogeneous layer with a fixed (phase) composition, visible as a plateau in the RBS spectra, is more prominent at

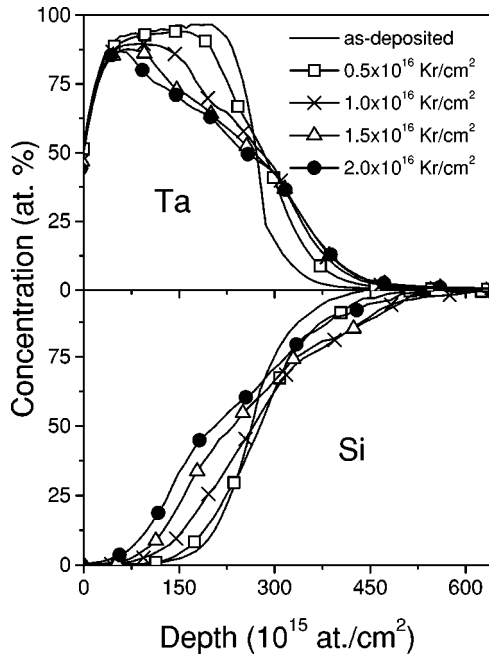


FIG. 3. Extracted concentration profiles of Ta and Si from the RUMP analysis.

increased substrate temperatures. Figure 4 shows RBS spectra taken after 475-keV Xe-ion irradiations at different temperatures. The implanted fluence was fixed at 1×10^{16} ions/cm². It is clearly seen that atomic mixing is observed at liquid-nitrogen temperature and is almost independent up to a temperature of 100 °C. After the irradiation at 200 °C, a plateau appears near the Ta/Si interface and the mixed region either contains a Ta-rich composition or a mixture of TaSi₂ and nonreacted Ta. When the irradiation temperature reached 400 °C, the composition at the interface region corresponded to the pure TaSi₂ phase and the composition near the surface region became Ta rich. In order to further elucidate the phase structure of the mixed region, we performed grazing-angle XRD analyses of all the samples irradiated at RT or LN₂ temperature.

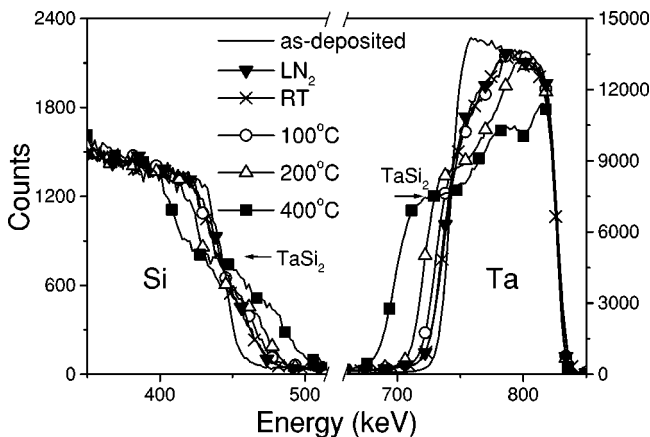


FIG. 4. RBS spectra taken before and after 475-keV Xe-ion irradiation of Ta (70 nm)/Si bilayers at different irradiation temperatures.

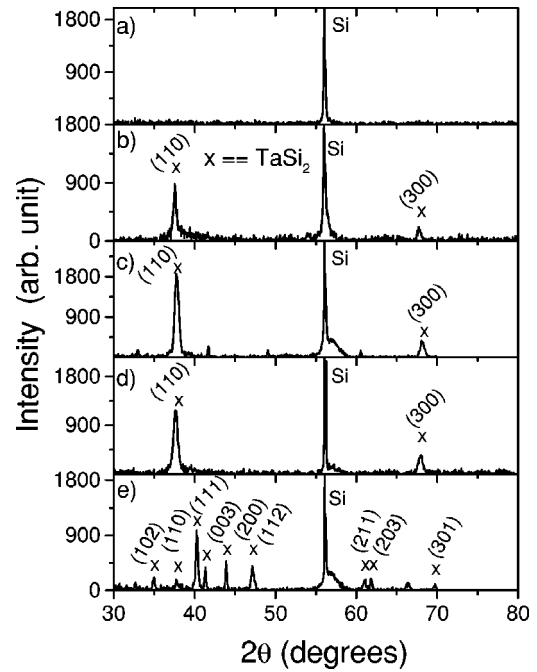


FIG. 5. XRD spectra of Ta/Si bilayers (a) as-deposited; after ion irradiation at RT, $\Phi = 2 \times 10^{16}$ ions/cm² (b) 120 keV Ar, (c) 400 keV Kr, (d) 475 keV Xe, (e) 475 keV Xe at 400 °C, $\Phi = 1 \times 10^{16}$ ions/cm².

D. Phase analysis

Diffraction spectra taken before and after Ar, Kr, and Xe irradiations at RT for a fluence of 2×10^{16} ions/cm² are displayed in Figs. 5(a)–5(d). The XRD spectrum [Fig. 5(a)] obtained from the as-deposited sample shows only the reflection from the single crystal Si(100) at 56°. This peak appears as the Bragg condition is satisfied for the incident angle of 3°. After irradiations, in all the cases the TaSi₂ phase is indeed produced during ion irradiation at RT. By way of additional XRD analysis, the fluence and temperature dependence of TaSi₂ phase formation were detected. For 475-keV Xe ions and LN₂ substrate temperature, only the TaSi₂ phase was identified when the ion fluence varied from 0.5 to 2×10^{16} ions/cm². Hence the formation of a Si-rich compound phase at RT or LN₂ temperature is purely due to the effects of ion-beam irradiation. In all these cases of irradiations at RT and LN₂, only two reflections from (110) and (300) planes were detected. But when the sample temperature increased to 400 °C during 475-keV Xe irradiations, XRD reflections from various planes of the TaSi₂ phase were registered and the spectrum is shown in Fig. 5(e). It may contain some other phases as some reflections could not be identified. This high-temperature-irradiated sample indicates a different microstructure compared to the RT and LN₂ samples and this can be attributed to the combined effects of thermal heating and ion beam. Phases synthesized by ion-beam irradiations at low temperatures in other metal/semiconductor systems are summarized in Table I.

E. Growth rate of the mixed layer

Quantitative information regarding the elemental redistribution across the bilayer interface is essential for understand-

TABLE I. The experimental mixing/reaction rates $\Delta\sigma^2/\Phi$ are compared with the values obtained from the compound formation model assuming local or global spikes.

Bilayer system	Z_{ave}	Ion species	Irradiation temperature	Ion-beam-induced phase	Deposited damage energy F_D (keV/nm)	Athermal mixing rate $\Delta\sigma^2/\Phi$				Ref.
						Experimental	Ballistic	Local	Global	
Ta/Si	43.5	Xe	RT, LN ₂	TaSi ₂	3.0	7.8±0.5	3.2	35	9.9	This work
	43.5	Kr	RT, LN ₂	TaSi ₂	2.5	6.4±0.5	2.7	29	6.9	This work
	43.5	Ar	RT	TaSi ₂	0.62	6.6±0.5	0.7	7.3	0.4	This work
	43.5	Ar	RT	TaSi ₂	0.47	4.6±0.4	0.5	5.5	0.3	This work
	43.5	Ar	RT	TaSi ₂	0.32	3.3±0.4	0.3	3.7	0.1	This work
Pd/Si	30	Au	LN ₂	Pd ₂ Si	4.4	31±3	4	49	33	10
Fe/Si	20	Xe	RT, LN ₂	Solid sol. and	2.8	4.8±0.5	0.5	4.0	3.5	18
	20	Ar	RT, LN ₂	γ -FeSi ₂	0.9	1.3±0.2	0.16	1.3	0.4	18
Ni/Si	21	Au	RT	Ni ₂ Si	4.8	11.8±1.0	2	9	10	10
Cu/Ge	31.5	Kr	RT	Cu ₃ Ge	1.6	21±2	2	20	4	11
	31.5	Ar	RT	Cu ₃ Ge	0.4	5.4±0.6	0.5	5	0.3	11
Ni/Ge	30	Kr	RT	Ni ₂ Ge	1.6	19±2	1.6	13	2.6	12
	30	Ar	RT	Ni ₂ Ge	0.5	5.6±0.5	0.5	4	0.3	12
Co/Ge	29.5	Kr	RT	Co ₂ Ge	1.5	7.7±0.8	0.8	6	1.2	13
	29.5	Ar	RT	Co ₂ Ge	0.4	1.6±0.2	0.2	1.6	0.1	13

ing the underlying mechanisms of ion-beam-induced mixing and reactions at low temperature. From the measured Ta or Si depth profiles, we deduced the increase of the variance σ^2 of the intermixed region as a function of the ion fluence, $\Delta\sigma^2(\Phi) = \sigma^2(\Phi) - \sigma^2(0)$, where $\sigma^2(0)$ and $\sigma^2(\Phi)$ are the variances before and after irradiation at a fluence Φ . For our calculation we assumed $\sigma^2 = 2\Omega^2$, where Ω denotes half the thickness of the interface zone in which the Ta (or Si) concentration changes from 84% to 16% of the bulk value. When determining $\Delta\sigma^2$, we assumed that the surface roughness of the samples for increased ion fluence did not change appreciably. The average atomic density of Ta and Si (5.25×10^{22} ions/cm³) was used for the depth scale. In Figs. 6(a)–6(c), the quantity $\Delta\sigma^2$ is plotted versus the ion fluence Φ for the three projectiles. In all cases, $\Delta\sigma^2$ varies linearly with Φ , providing the well-defined slopes $\Delta\sigma^2/\Phi$, labeled as the mixing rate. In addition, Figs. 6(b) and 6(c) show that the mixing rates at LN₂ and RT almost agree with each other. Evidently, neither the radiation-enhanced nor temperature difference plays a role at these temperatures. A linear growth of the mixed layer had previously been observed in many other metal/semiconductor systems, such as Fe/Si, Pd/Si, Ni/Si, Cu/Ge, etc., which had been subjected to ion irradiations.^{10–13,18} For many of these systems, the variance $\Delta\sigma^2$ was found to vary linearly with the annealing time during thermal treatment at a fixed temperature.^{1,5} This process is referred to as diffusion controlled, which also appears to apply to these cases of ion-beam irradiation. From the linear regression analysis, the mixing rates $\Delta\sigma^2/\Phi$ obtained for all the cases are summarized in Table I. For comparison, the mixing rates obtained for several other metal/semiconductor systems,^{10–13,18} e.g., Fe/Si, Ni/Si, Cu/Ge, Ni/Ge, Co/Ge, and Pd/Si, are also given in Table I. In all these systems, except the Pd/Si bilayer,¹⁰ $\Delta\sigma^2(\Phi)$ was found to be proportional to

the implanted fluence Φ . Table I shows that the mixing rate increases with increasing ion mass and deposited energy F_D . The linear dependence of the mixing rate on the deposited energy in the case of the Ta/Si system irradiated with Ar ions is illustrated in Fig. 7, giving the mixing efficiency

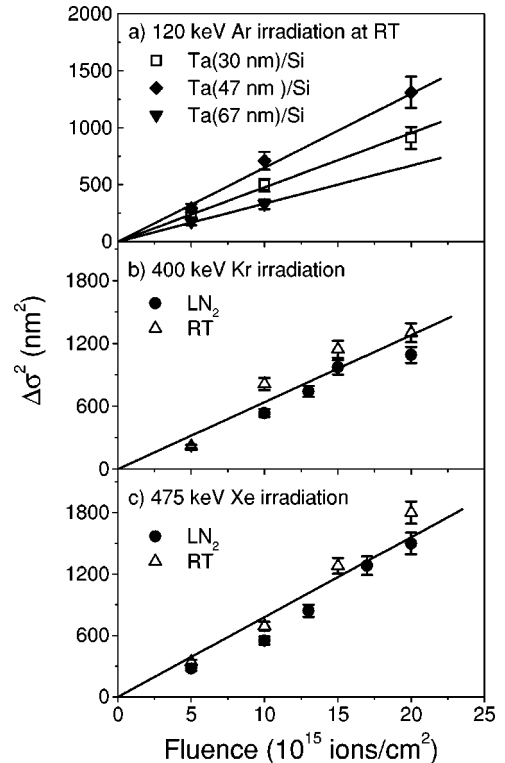


FIG. 6. Increase of the variance of the mixed interface layer as a function of the ion fluence Φ (a) 120 keV Ar, (b) 400 keV Kr, and (c) 475 keV Xe.

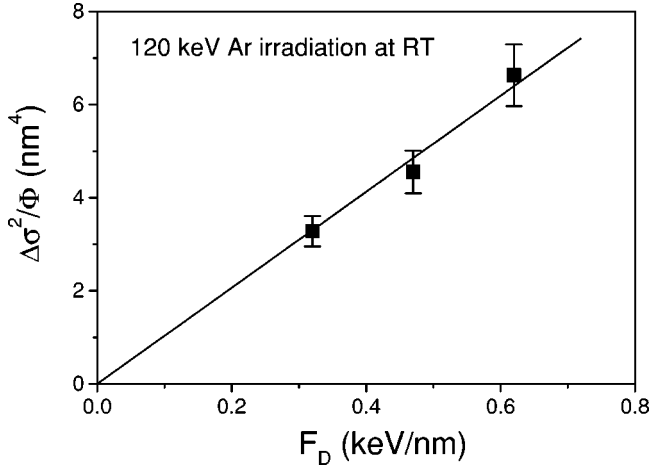


FIG. 7. Variation of the mixing rate as function of the deposited damage energy F_D due to 120-keV Ar irradiation at the Ta/Si bilayer interface.

$\Delta\sigma^2/\Phi F_D = 10 \pm 1 \text{ nm}^5/\text{keV}$. Such a linear dependence of the mixing rate on F_D was also observed in the Cu/Ge, Co/Ge, and Ni/Ge systems.^{11–13}

IV. DISCUSSION

The underlying physical processes involved during ion irradiation may be inferred from the functional dependence of the interface broadening $\Delta\sigma^2$ on the ion fluence Φ , the deposited energy F_D , and the irradiation temperature.^{7–11,25} It is generally observed that the mixing rate is independent of temperature during low-temperature irradiations. Temperature-dependent mixing,⁷ such as radiation-enhanced diffusion, is activated above a critical temperature T_c which can be estimated from the relation $T_c = 100\Delta H_{\text{coh}}$, as demonstrated by Cheng.⁹ Here ΔH_{coh} is the average cohesive energy of the bilayer system.²⁶ In the present case, T_c should be around 350 °C. The present experimental results of Ta/Si do not show (see Fig. 4) any influence of the irradiation temperature up to 100 °C. We conclude that the mixing effect is insensitive to the irradiation temperature in this temperature range. Several phenomenological models^{7–11,25} have been proposed to explain athermal mixing and phase formation at the interfaces of bilayers. These models may be classified on the basis of the microstructure of the intermixed region. If the mixed region is a solid solution, one may either apply the ballistic model,²⁵ which considers only the kinematics of the binary collisions, or thermal spike models, which take into account the chemically guided atomic diffusion under local⁸ or global⁹ thermal spikes. On the other hand, for the mixed region consisting of a compound phase, compound formation models have been developed which assume atomic diffusion guided by a chemical driving force due to compound formation, either under the ballistic condition¹⁰ or in the presence of local¹¹ or global¹⁰ thermal spikes. By means of the fractal geometry approach, Cheng⁹ showed that the ballistic process should dominate in binary systems with an average element number of $Z_{\text{ave}} < 20$, and for $Z_{\text{ave}} > 20$ thermal spikes become dominant. In the present

case of Ta/Si bilayers, the average element number $Z_{\text{ave}} = 43.5$ suggests thermal spikes to be effective. We will now discuss the mixing rates under three different assumptions, i.e., ballistic, local and global spikes. According to the pure ballistic model²⁵ by Sigmund and Gras Marti, the mixing rate is defined as

$$k_{\text{ball}} = \Delta\sigma^2/\Phi = \frac{1}{3} \Gamma_0 \xi \frac{F_D R_d^2}{NE_d}, \quad (1)$$

where $\Gamma_0 = 0.608$ is a dimensionless constant, ξ a kinematic factor, F_D the average damage energy deposited at the interface, N the average atomic density, E_d the displacement energy, and R_d the minimum separation distance (about 1 nm) for producing a stable Frenkel pair.^{7–9} The calculated ballistic mixing rates for the Ta/Si system are by one to two orders of magnitude (not given in Table I) lower than the experimental values. This is also true for the other metal/semiconductor systems summarized in Table I. Therefore, pure ballistic mixing contributes very little to the overall mixing rate in such highly reactive systems.

As mentioned before, thermal spikes, along with chemical driving forces, play a dominant role in the mixing process for systems with $Z_{\text{ave}} > 20$. The influence of the chemical driving forces depends on the nature (compound or solid solution) of the mixed region and is more pronounced^{10,11} when the mixed region is a compound phase. Ion-beam-induced formation of crystalline silicide and germanide phases was observed in many metal/Si and metal/Ge systems,^{7,10–14,18} the metal-rich phases often being predominant. For example, a mixture (determined by Mössbauer analysis) of Fe-Si solid solution and silicide phases (mainly γ -FeSi₂) forms during RT or LN₂ irradiation of 40-nm ⁵⁷Fe/Si bilayers with 250-keV Xe or 100-keV Ar ions,¹⁸ while at 400–600 °C a mixture of a FeSi and β -FeSi₂ is formed.¹⁷ In the Cu/Ge system,¹¹ the low-resistivity Cu₃Ge compound was obtained during RT irradiations with 1-MeV Kr or Ar ions. Extensive experimental and theoretical efforts have been made to understand the effects of thermodynamic driving forces and kinetics in the phase formation processes.^{7,27} A set of empirical rules has been proposed,²⁷ which predict evaluation of the phases formed under ion bombardment. Among the many factors influencing the final phase(s) to be formed, we mention the structure and complexity of this phase, the width of the phase fields, the heat of formation, and the substrate temperature.

Since we observed the formation of compounds during ion-beam mixing and the thermal spikes to be predominant in all the cases, we applied the compound formation models^{10,11} under thermal spikes. Differentiating between local and global spikes, local spikes generally develop below a critical deposition energy F_{DC} above which global spikes form. Unfortunately, for many cases the value of F_{DC} is not known: hence, we applied both models.

Assuming the compound $A_a B_b$ (for example, TaSi₂) to be formed at the A/B interface (where $A = \text{Ta}$ and $B = \text{Si}$) during ion-beam irradiation, the athermal mixing rate^{10,11} can be written as

$$\frac{\Delta\sigma^2}{\Phi} = k_{\text{mix}} f_{\text{comp}}, \quad (2)$$

where the enhancement factor f_{comp} due to compound formation is given by

$$f_{\text{comp}} = 2 \left[\frac{C_A}{aC/(a+b)} + \frac{C_B}{bC/(a+b)} \right], \quad (3)$$

where C_A , C_B , and C are the atomic densities of elemental A , B , and their compound A_aB_b . For the factor k_{mix} we have used the expression derived for either local spikes,^{8,11}

$$k_{\text{mix}} = \frac{K_s Z_{\text{ave}}^{1.77} F_D}{C^{2/3} \Delta H_{\text{coh}}^2}, \quad (4)$$

or global spikes,^{7,10}

$$k_{\text{mix}} = \frac{K_1 F_D^2}{C^{5/3} \Delta H_{\text{coh}}^2}. \quad (5)$$

For the Ta/Si system, we considered the formation of tantalum silicide phases in all the cases through the reaction $\text{Ta} + 2\text{Si} \rightarrow \text{TaSi}_2$. The parameters used for the calculations are as follows: $K_s = 0.9 \times 10^{-6} \text{ nm}^3 \text{ keV}$,¹¹ $K_1 = 0.0035 \text{ nm}$,^{9,10} Z_{ave} = average atomic number = 43.5, $C_A = 5.55 \times 10^{22} \text{ atoms/cm}^3$ = atomic density of Ta, $C_B = 5.00 \times 10^{22} \text{ atoms/cm}^3$ = density of Si, and $C = 5.18 \times 10^{22} \text{ atoms/cm}^3$ that of TaSi_2 ; $\Delta H_{\text{coh}} = 6.4 \text{ eV/atom}$ is the average cohesive energy²⁶ of Ta/Si. Furthermore, knowledge of the moving species participating in the reaction is important. If both Ta and Si are about equally mobile, both terms inside Eq. (3) must be retained. Since thermal spikes create a very high local temperature, information on the atomic mobility may be inferred from thermal diffusion experiments. Many studies^{1,5,28} gave evidence that during thermally induced refractory-metal silicide formation, Si would be the predominant moving species at low temperatures (<800 °C), while metal atoms would also become mobile at higher temperatures. When assuming that in all the cases both Ta and Si are mobile during the spike phase, we arrive at the mixing rates listed in Table I. It may be noted that the purely ballistic model [Eq. (1)] also predicts a linear dependence of the mixing rate on F_D . Therefore, it would be interesting to calculate the mixing rate after introducing the compound enhancement factor f_{comp} [Eq. (3)] in the purely ballistic model given in Eq. (1). The compound enhancement factor is the same for the linear collision and thermal spike regimes. The calculated results obtained from this compound ballistic model are compared in Table I. The results from other metal/semiconductor systems are also summarized in Table I. A comparison of experimental and model mixing rates in the various systems provides some very interesting conclusions. Compound formation under ballistic conditions can be safely excluded, as the calculated mixing rates are about 3–10 times lower than the experimental ones. The compound formation model under local spikes [Eq. (4)] reproduces well all the mixing rates for the Ar irradiations in the metal/Si sys-

tems (Ta/Si, Fe/Si) as well as the mixing rates of the Ar and Kr irradiations in the metal/Ge systems (Cu/Ge, Co/Ge, and Ni/Ge). The results for the heavy ion irradiations of Fe/Si (Xe) and Ni/Si (Au) bilayers can be explained by either local or global spikes. In the case of Kr- and Xe-irradiated Ta/Si and Au-irradiated Pd/Si bilayers, the mixing rates are only reproduced when assuming global spikes [Eq. (5)]. It appears that one of the decisive parameters to distinguish between local and global spikes in metal/Si and metal/Ge bilayers is the damage energy F_D deposited at the interface: for $F_D < 2.5 \text{ keV/nm}$, local spikes are formed, giving rise to phase formation, while for $F_D > 2.5 \text{ keV/nm}$, global spikes enhance the growth. The role of the other parameter Z_{ave} , which varies between 20 and 43.5 and, of course, also enters the density of defects in the collision cascade, cannot be clearly established from the present data set. For the sake of completeness, if we use purely local and global spike models [Eq. (4) or (5) together with a factor ‘‘ $1 + K_2 \Delta H_{\text{mix}} / \Delta H_{\text{coh}}$ ’’ which appears to be due to a solid solution approximation; ΔH_{mix} is the heat of mixing or heat of formation and K_2 is a constant^{8,9]}, the calculated mixing rates also become one order of magnitude smaller than the experimental results (not shown in Table I). Therefore, these results demonstrate that the mechanisms of ion-beam-induced mixing and compound formation in highly reactive metal/semiconductor systems are governed by strong chemical driving forces.

V. CONCLUSIONS

We have investigated atomic mixing and TaSi_2 phase formation at the Ta/Si interface, due to noble-gas (Ar, Kr, and Xe) ion irradiations at temperatures between LN_2 and 400 °C. The thickness of the intermixed region was found to increase rapidly either with ion mass, ion fluence, or sample temperature. In all cases (RT and LN_2), the variance $\Delta\sigma^2$ of the mixed/reacted layer increased proportionally to the ion fluence Φ . The measured athermal mixing/reaction rates, which experimentally are in the range $\Delta\sigma^2/\Phi = 3\text{--}8 \text{ nm}^4$, were explained with the help of a compound formation model in the presence of thermal spikes. Purely ballistic mixing can be ruled out to govern the mixing process. When increasing the ion mass from Ar to either Kr or Xe, a transition from local spikes to global spikes was observed. It was connected to a critical damage energy of about $F_D = 2.5 \text{ keV/nm}$ deposited at the interface. It is satisfying to see that this critical energy density also differentiates between local and global spikes in many other reactive metal/Si or Ge systems, which are listed in Table I. According to Eqs. (4) and (5), there should be a clear distinction between local and global spikes on the basis of the F_D dependence of the mixing rate $\Delta\sigma^2/\Phi$, which should vary proportionally to F_D in the case of local spikes and to F_D^2 in the case of global spikes. An experimental verification of this effect still appears to be missing. Another point to be investigated in more detail is the transition between atomic mixing and phase for

mation as a function of the ion fluence Φ . It is quite clear that the XRD analysis is not able to monitor this transition. For that reason, we are performing more ion beam mixing studies on $^{57}\text{Fe}/\text{Si}$ bilayers using highly enriched ^{57}Fe top layers and conversion electron Mössbauer spectroscopy to measure the phase composition.

ACKNOWLEDGMENTS

The authors are grateful to Detlef Purschke for expertly running the IONAS accelerator and to Professor Wolfgang Bolse for useful comments on the models used. This work has been supported by DFG and BMBF.

*Corresponding author. Electronic address: dhar@physik2.uni-goettingen.de

- ¹A. H. Reader, A. H. van Ommen, P. J. W. Weijs, R. A. M. Wolters, and D. J. Oostra, *Rep. Prog. Phys.* **56**, 1397 (1992).
- ²R. Pretorius, C. C. Theron, A. Vantomme, and J. W. Mayer, *Crit. Rev. Solid State Mater. Sci.* **24**, 1 (1999).
- ³Ch. Buchal, M. Löken, Th. Lipinsky, L. Kappius, and S. Mantl, *J. Vac. Sci. Technol. A* **18**, 630 (2000).
- ⁴D. Leong, M. Harry, K. J. Reeson, and K. P. Homewood, *Nature (London)* **387**, 686 (1997).
- ⁵F. M. d'Heurle and P. Gas, *J. Mater. Res.* **1**, 205 (1986).
- ⁶A. Vantomme, S. Degroote, J. Dekoster, G. Langouche, and R. Pretorius, *Appl. Phys. Lett.* **74**, 3137 (1999).
- ⁷M. Nastasi and J. W. Mayer, *Mater. Sci. Eng., R.* **12**, 1 (1994).
- ⁸W. Bolse, *Mater. Sci. Eng., R.* **12**, 53 (1994); *Mater. Sci. Eng., A* **253**, 194 (1998).
- ⁹Y.-T. Cheng, *Mater. Sci. Rep.* **5**, 45 (1990).
- ¹⁰J. Desimoni and A. Traverse, *Phys. Rev. B* **48**, 13 266 (1993).
- ¹¹S. Dhar, Y. N. Mohapatra, and V. N. Kulkarni, *Phys. Rev. B* **54**, 5769 (1996).
- ¹²S. Dhar, T. Som, and V. N. Kulkarni, *J. Appl. Phys.* **83**, 2363 (1999).
- ¹³S. Dhar, Ph.D. thesis, I.I.T. Kanpur, India, 1997.
- ¹⁴L. Rissanen, S. Dhar, and K. P. Lieb, *Phys. Rev. B* **63**, 155411 (2001).
- ¹⁵L. Rissanen, S. Dhar, K. P. Lieb, K. J. Engel, and M. Wenderoth, *Nucl. Instrum. Methods Phys. Res. B* **161-163**, 990 (2000).
- ¹⁶S. Dhar, M. Milosavljevic, N. Bibic, and K. P. Lieb, *Phys. Status Solidi B* **222**, 295 (2000).
- ¹⁷M. Milosavljevic, S. Dhar, N. Bibic, P. Schaaf, M. Han, and K. P. Lieb, *Appl. Phys. A: Mater. Sci. Process.* **71**, 43 (2000).
- ¹⁸S. Dhar, N. Bibic, K. P. Lieb, M. Milosavljevic, and P. Schaaf (unpublished).
- ¹⁹A. Dobrosavljevic, M. Milosavljevic, N. Bibic, and A. Efremov, *Rev. Sci. Instrum.* **71**, 786 (2000).
- ²⁰M. Uhrmacher, K. Pampus, F. J. Bergmeister, D. Purschke, and K. P. Lieb, *Nucl. Instrum. Methods Phys. Res. B* **9**, 234 (1985).
- ²¹J. F. Ziegler, J. P. Biersack, and U. Littmark, *The Stopping and Range of Ions in Solids* (Pergamon, New York, 1985).
- ²²K. P. Lieb, *Contemp. Phys.* **40**, 385 (1999).
- ²³L. R. Doolittle, *Nucl. Instrum. Methods Phys. Res. B* **9**, 344 (1985).
- ²⁴N. P. Barradas, C. Jeynes, and R. P. Webb, *Appl. Phys. Lett.* **71**, 291 (1997).
- ²⁵P. Sigmund and A. Gras Marti, *Nucl. Instrum. Methods Phys. Res. B* **182/183**, 25 (1981).
- ²⁶C. Kittel, *Introduction to Solid State Physics* (Wiley, New York, 1976).
- ²⁷G. S. Was, *Prog. Surf. Sci.* **32**, 211 (1990).
- ²⁸I. J. Raaijmakers, A. H. Reader, and P. H. Oosting, *J. Appl. Phys.* **63**, 2790 (1988).